PROCEEDINGS, 51st Workshop on Geothermal Reservoir Engineering
Stanford University, Stanford, California, February 9-11, 2026
SGP-TR-230

Optimization of Well Trajectory and Stimulation Design for Well 16C(78)-32 to Enhance Multi-Well Connectivity at Utah FORGE

PeiJian Li[1], Pengju Xing[2,3], John McLennan[1,2]

[1]Department of Chemical Engineering, University of Utah

[2]Energy & Geoscience Institute, University of Utah

[3]Department of Civil and Environmental Engineering, University of Utah

Peijian.Li@utah.edu

Keywords: Enhanced Geothermal Systems, fluid rheology, fracture hits, interwell connectivity, proppant settlement, stress shadowing

ABSTRACT

Fracture connectivity optimization and long-term circulation performance are crucial for Enhanced Geothermal Systems (EGS) success. This research assesses various stimulation design choices for a future well, Well 16C(78)-32, at the Utah FORGE location through a numerical sensitivity analysis. This well would be placed to the north of the existing well pair (600 ft at the heel and 280 ft at the toe). The analysis explores the combined impacts of lateral and vertical positioning, stimulation fluid type, and previous stimulation activities. Three trajectory options were examined: elevation alignment with Well 16A(78)-32, a mid-level elevation placement between the two wells, and elevation alignment with Well 16B(78)-32, all cases offset to the north. Each trajectory was assessed with crosslinked CMHPG and slickwater treatments, with and without considering the 2024 FORGE stimulation history.

Simulated fracture hits at Wells 16A and 16B were analyzed to assess hydraulic connectivity and fracture extension. The findings reveal that the vertical positioning significantly influences interwell connectivity, with mid-level placement yielding a more balanced and resilient fracture network. Crosslinked CMHPG provides more balanced and durable interwell connectivity under both unstimulated and stimulated stress conditions.

Analysis of proppant settlement reveals the significance of wellbore connectivity supported by proppant in maintaining interwell communication during circulation. Continuous propped pathways between wells are crucial for sustaining effective connectivity and reduce reliance on isolated fracture segments. Large treatment designs with crosslinked CMHPG can improve interwell connectivity. Therefore, a robust design option for future EGS development at FORGE involves a mid-level trajectory for Well 16C(78)-32 combined with a crosslinked CMHPG stimulation strategy.

1. INTRODUCTION

Enhanced Geothermal Systems (EGS) are considered to be a critical technology for large scale low carbon baseload energy generation from deep, low permeability, high temperature crystalline reservoirs. Economical heat extraction is not dependent on natural permeability or fluid circulation, rather on the creation and management of subsurface flow pathways via hydraulic stimulation. (US Department of Energy, 2019)[9]. Thus, long-term performance of an EGS reservoir depends not only on initiating fractures, but also on maintaining hydraulic connectivity, fracture conductivity and thermally efficient circulation between multiple wells.

Optimizing well spacing in EGS is vital for thermal efficiency and interwell connectivity. Closer spacing improves connectivity, but faster breakthroughs lead to rapid cooling and lower efficiency. Larger spacing improves heat exchange and thermal sustainability but requires higher injection pressures. Good spacing design is essential for efficient and sustainable geothermal energy production (Podgorney et al., 2023)[7].

The EGS performance depends on the structure of the fracture network, such as number of fractures, fracture spacing, width and hydraulic conductivity. These factors play an important role in the flow between injection wells and production wells, and thermal energy extraction efficiency (Asai et al., 2018)[1].

Predicting and managing connectivity between injector and producer wells is a key technical hurdle for EGS implementation, especially for projects focusing on long-term circulation rather than short-duration injection tests. The Utah Frontier Observatory for Research in

Geothermal Energy (FORGE) was established by the U.S. Department of Energy to address these challenges through a dedicated, instrumented field laboratory for advancing EGS research and engineering (Moore et al., 2020)[6].

Hydraulic stimulation campaigns conducted at Utah FORGE have provided important insights into fracture initiation, propagation, and interwell hydraulic communication in crystalline rock (Moore et al. 2023[5]; England et al. 2025[2]). Early stimulations in Well 16A(78)-32 showed that stimulation fluid rheology plays a significant role in fracture geometry and pressure response even when injection rates and volume are comparable. Stimulation campaigns with proppant also showed that fracture width and conductivity must be maintained for long term hydraulic connectivity (McClure 2023[3]; McClure et al. 2024[4]).

The drilling and stimulation of a second deviated well, 16B(78)-32, allowed for direct observation of interwell connectivity at Utah FORGE. Pressure communication, fiber-optic monitoring, and frac-hit observations confirmed that hydraulic fractures from Well 16A(78)-32 can intersect Well 16B(78)-32 and connect Well 16B(78)-32, although connection "strength" and distribution differ depending on stimulation stage, fluid system, well placement and well spacing. These results showed that previously adopted injector–producer design paradigms cannot assume interwell connectivity based on well spacing or vertical offset but must be planned through coordinated trajectory placement and stimulation design.

The circulation test at Utah FORGE confirmed connection between injection well 16A(78)-32 and production well 16B(78)-32 by the hydraulic fracture/natural fracture network. Balanced connectivity is crucial for efficient heat extraction while minimizing localized thermal degradation, pressure buildup, rapid fluid transit, and premature thermal breakthrough (Xing et al., 2024)[11].

Well 16C(78)-32 is the third deviated well in the Utah FORGE reservoir and represents a significant step toward true multi-well EGS system development. Instead of fixed injector or producer roles, FORGE triplet concept emphasizes flexibility, allowing any well to function as injector or producer under different circulation conditions, study the direction flow behavior, thermal sweep efficiency, and fracture control circulation performance and impose new demands on trajectory optimization and stimulation robustness.

The Well 16C(78)-32 design therefore requires more than well placement. The question is how should 16C(78)-32 be placed relative to existing wells to ensure balanced connectivity, how sensitive to stimulation fluid rheology, and which configurations can best withstand stress shadowing and long-term circulation demands. Addressing these questions before drilling is essential to reduce risk and to ensure future circulation experiments produce stable results.

This paper presents a forward-looking numerical study to improve the trajectory and stimulation design of Well 16C(78)-32. Using a ResFrac[8] modeling framework calibrated to the 2024 Utah FORGE stimulation campaign, three candidate well trajectories are studied with 4 stimulation sensitivity cases based on fluid rheology and previous stimulation effects. Fracture connectivity and proppant settlement are investigated. By synthesizing validated physical mechanisms into a design-oriented framework, this paper provides actionable guidance to multi-well EGS development at FORGE and contributes to the goal of scaling up geothermal energy deployment in crystalline reservoirs.

2. UTAH FORGE BACKGROUND

The Utah FORGE site is located near Milford, Utah, adjacent to the Mineral Mountains, and targets a hot, low-permeability granitic reservoir at depths greater than 2 km. Temperatures in the target interval are close to 240°C. The reservoir has limited natural permeability and requires hydraulic stimulation to establish circulation pathways (Moore et al., 2023)[5]. Well 16A(78)-32 was drilled at an angle of around 65° and served as the injection well during multiple stimulation and circulation campaigns. Well 16B(78)-32 was drilled above 16A(78)-32 to intersect a zone of induced microseismicity resulting from a 2022 stimulation program. The 2024 stimulation campaign used slickwater and crosslinked CMHPG fluids, providing a rich data set for evaluation of the effects of fluid rheology on stimulation results.

3. CONCEPTUAL DIRECTIONAL DESIGN FOR WELL 16C(78)-32

3.1 Design objectives and planning philosophy

The design of Well 16C(78)-32 extends hydraulic stimulation and circulation knowledge obtained from Wells 16A(78)-32 and 16B(78)-32 at Utah FORGE. The goal is to improve interconnectivity between multiple wells while preserving safety and compliance with land, spacing, and drilling constraints.

The design aims to:

1. Maximize connection between the new well (16C(78)-32) and the injector-producer pair (16A-16B) to improve fracture intersection and pressure communication.

2. Maintain sufficient separation from existing wells (including legacy vertical and deviated wells) to eliminate collision and minimize interference risks.

3. Maintain flexibility for future operations such as stage stimulation, multi-well circulation tests, thermal breakthrough experiments and long-term reservoir characterization.

Well 16C(78)-32 will have the same inclination angle (65°) as Wells 16A(78)-32 and 16B(78)-32, but with different heel and toe lateral offset. The initial suggestion includes a heel spacing of 600 feet and a toe spacing of 200 to 300 feet (see Figure 1). Two trajectory options were considered:

1) Placing 16C(78)-32 south of 16A(78)-32 and 16B(78)-32

2) Placing 16C(78)-32 north of 16A(78)-32 and 16B(78)-32

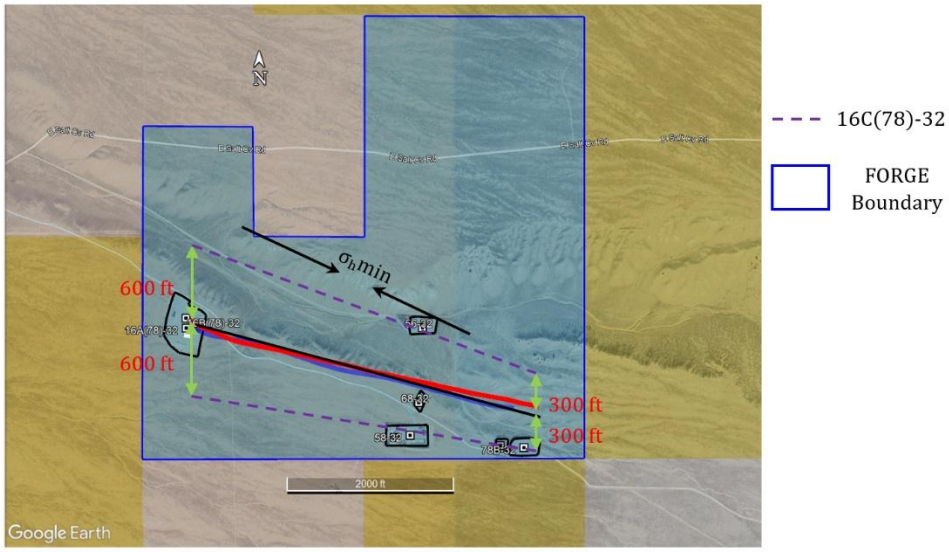

Figure 1. Schematic of Well 16C(78)-32. The purple dashed line is the potential Well 16C(78)-32 trajectory.

3.1.1 Southern Placement Risks

Placing Well 16C(78)-32 south of existing wells leads to several technical and operational risks:

- Lease boundary risk: fracture propagation from stimulation stages near the toe of a southern lateral may extend beyond FORGE lease boundary and can diminish control of seismicity and possibly violate regulatory requirements.
- Well interference risk: southern placement increases proximity to wells such as 58-32 and 78B-32 and increases collision risk in drilling and interference potential in stimulation.
- Stress misalignment: southern direction has greater misalignment of well trajectory to the minimum horizontal stress direction (σ_{hmin}) may hinder fracture initiation and propagation and increase hydraulic stimulation difficulty.

3.1.2 Advantages of Northern Placement

In contrast, placing Well 16C(78)-32 north of Well 16A(78)-32 and 16B(78)-32 has advantages (Figure 1):

- Improved fracture containment within FORGE lease boundary.
- Closer alignment with σ_{hmin}, allowing effective fracture initiation and predictable lateral growth.
- Reduced well interference complexity, only one nearby deep well (Well 56-32) needs specific mitigation/consideration.

Based on these considerations, north-side placement was chosen as the preferred configuration for all conceptual trajectory scenarios considered in this paper.

3.2 Conceptual Trajectory Scenarios

After picking the north-side position, three conceptual trajectory scenarios were developed to evaluate the effect of vertical positioning on hydraulic connectivity, fracture propagation behavior and stimulation efficiency.

The scenarios are:

A: Vertical alignment with Well 16A(78)-32 in the lower reservoir interval (Figure 2),

B: Mid-level placement between Wells 16A(78)-32 and 16B(78)-32 (Figure 3),

C: Vertical alignment with Well 16B(78)-32 in the upper reservoir interval (Figure 4).

In all scenarios, Well 16C(78)-32 is drilled sub-parallel to the existing laterals in both inclination and azimuth to maintain the same stress orientation. Minor azimuth adjustments were applied to each trajectory to satisfy anti-collision requirements with the nearby deep well 56-32 while maintaining close alignment with the regional minimum horizontal stress direction. Map-View lateral layouts for all trajectory scenarios are summarized in Appendix A.

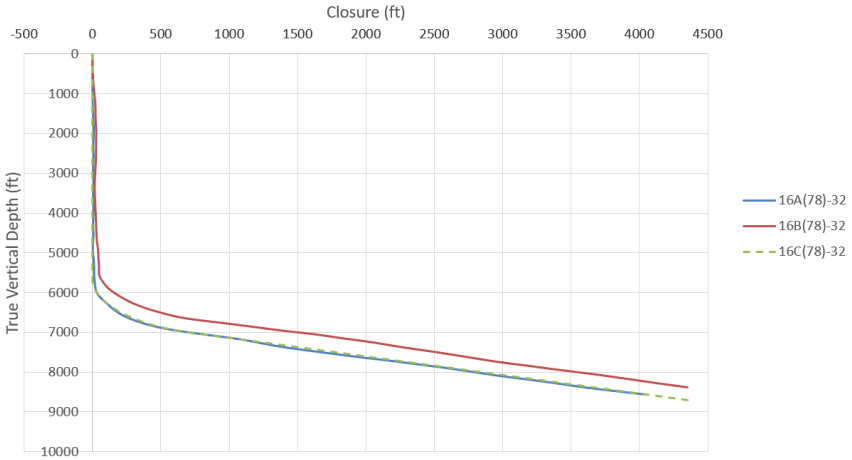

Figure 2. Full directional trajectory of Well 16C(78)-32 for Scenario A, showing alignment with Well 16A(78)-32 and consistency with the target depth envelope.

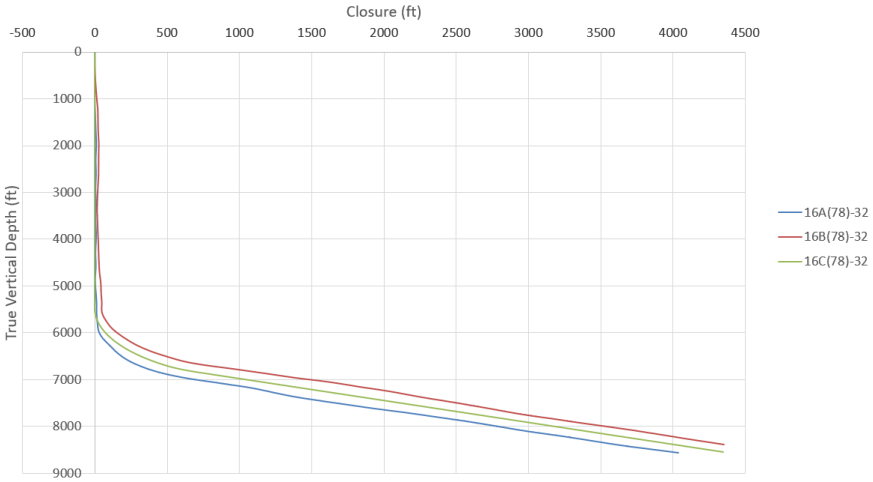

Figure 3. Full directional trajectory of Well 16C(78)-32 for Scenario B, illustrating mid-level placement between Wells 16A(78)-32 and 16B(78)-32 and consistency with the target depth envelope.

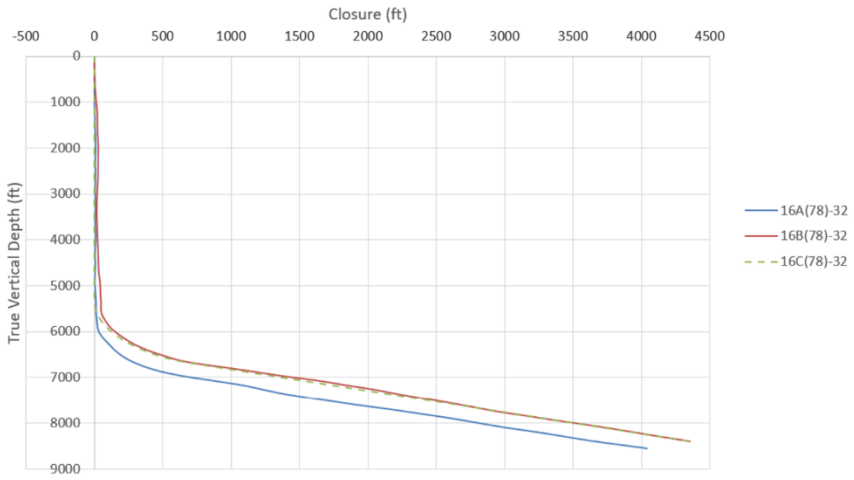

Figure 4. Full directional trajectory of Well 16C(78)-32 for Scenario C, showing alignment with Well 16B(78)-32 and consistency with the target depth envelope.

4. NUMERICAL METHODOLOGY

4.1 Base model initialization and calibration

Numerical modeling for Well 16C(78)-32 was performed using ResFrac[8], a fully coupled hydraulic fracturing simulator which could represent fracture propagation, reservoir flow, geomechanics, thermal effects, and proppant transport all in one framework.

4.1.1 Formation and reservoir parameter initialization

The base numerical model was initialized using site-specific geological, mechanical and thermal properties representing the Utah FORGE granitic basement. Formation properties were obtained from FORGE modeling work of Xing et al. (2022)[10] and McClure et al. (2023)[3], which combine core measurements, diagnostic injection tests, stimulation observations, and microseismic interpretation. These parameters provide consistent and physically constrained basis for simulation of hydraulic fracture growth and fluid–rock interactions under EGS.

The base input parameters used in the ResFrac simulations are summarized in Table 1.

Table 1. Numerical simulation input parameters used for base model initialization.

Permeability	0.03 md	Formation compressibility	1x 10^{-5} psi^{-1}
Porosity	3%	Fracture gradient	0.73 psi/ft
Rock density	161 lb_m/ft^3	Rock heat capacity	0.239 BTU (lb-R)
Thermal conductivity	1.445 BTU (hr-ft-R)	Coefficient of linear thermal expansion	5.56x10^{-6}/°F
Biot coefficient	0.35	Horizontal fracture toughness	1630 psi-in $^{1/2}$
Pore pressure gradient	0.41 psi/ft	Vertical fracture toughness	1520 psi-in $^{1/2}$
Poisson's ratio	0.29	Young's modulus	5 x 10^6 psi
Surface temperature	68°F	Proppant grain diameter 100 mesh	150-200 microns
Crosslinked gel decay rate constant	0.67 hr^{-1}	Proppant grain diameter 40/70 mesh	212-420 microns

4.1.2 Fracturing fluid representation

Two representative fracturing fluid systems were modeled in this paper: a crosslinked CMHPG fluid and a slickwater fluid, reflecting the range of viscosities used in Utah FORGE stimulation operations. Fluid rheology was performed in ResFrac using apparent viscosity values representative of fracture-scale shear conditions.

Chemical rheology measurements were performed by Calfrac Well Services as part of 2024 Utah FORGE stimulation. Apparent viscosity was measured in temperature range (200–350°F) and shear rates. Results showed gradual reduction at high temperature due to thermal degradation. Based on estimated bottomhole fracture temperatures approaching 350°F and representative shear rate of 170 s^{-1}, apparent viscosity of 67.9cP was chosen for CMHPG numerical simulation. Time dependent viscosity loss was captured by first order gel decay reaction which allowed crosslinked fluid to gradually drop to lower viscosity state when pumping.

The slickwater was represented by an apparent viscosity of 0.45 cP at 170 s^{-1} consistent with published FORGE modeling and typical downhole slickwater behavior (McClure 2023)[3].

Fluid rheology was fully coupled with fracture geometry, pressure evolution and proppant transport in ResFrac, which allowed realistic simulation of fracture width development and transport efficiency under different viscosity conditions.

4.1.3 Base model calibration using field pressure data

The base model was calibrated by comparing pressure history to the 2024 hydraulic stimulation data from Well 16A(78)-32 (Stage 8 treated with crosslinked CMHPG and Stage 9 treated with slickwater). This calibration ensured forward simulations for Well 16C(78)-32 were based on physically verified fracture and reservoir parameters. The calibration focused on reproducing observed fracture initiation pressures and pressure evolution over stable propagation. The model captured different pressure responses between two fluid systems, indicating confidence in its prediction capability for forward simulations.

4.2 Sensitivity matrix and stimulation simulation setup

The deviated lateral of Well 16C(78)-32 was divided into 20 stimulation stages, each approximately 200 feet in length to evaluate fracture propagation, proppant placement and interwell hydraulic connectivity under different stimulation conditions. Each stage had four perforation clusters, spaced at 50 feet apart (from center to center), with a perforation design of 6 shots per foot, 3 feet per cluster, and 0.40” perforation diameter. This was kept constant in all simulations for the effects of fluid system selection and reservoir stimulation.

A sensitivity matrix was developed to assess the interwell connectivity and stress-shadow effects of fracturing fluid rheology and stimulation. Four stimulation cases were simulated for each trajectory scenario:

- Crosslinked CMHPG without prior stimulation on Wells 16A(78)-32 and 16B(78)-32
- Crosslinked CMHPG with prior stimulation on Wells 16A(78)-32 and 16B(78)-32
- Slickwater without prior stimulation on Wells 16A(78)-32 and 16B(78)-32
- Slickwater with prior stimulation on Wells 16A(78)-32 and 16B(78)-32

All stimulation treatments were pumped from Well 16C(78)-32. Pressure and fracture-driven hydraulic responses were measured at offset wells 16A(78)-32 and 16B(78)-32 for interwell connectivity and stress shadow effects.

To maximize the likelihood of hydraulic fracture connectivity and to maintain the consistency of available field observations, three stimulation treatment schedules were chosen for numerical analysis (Appendix B). They represent the range of stimulation treatments used in the 2024 Utah FORGE campaign and provide the same basis for scenario comparison.

Crosslinked CMHPG treatment schedule 1 (Table B1, Appendix B) represents the crosslinked CMHPG stimulation applied in the scenario analyses. This schedule was executed during Stage 8 stimulation of Well 16A(78)-32 in 2024, which represents the largest proppant volume and most aggressive CMHPG treatment performed at Utah FORGE to date.

The Slickwater Treatment Schedule (Table B2, Appendix B) was derived from the Stage 9 stimulation design for Well 16A(78)-32 (2024 FORGE campaign). The original Stage 9 design mirrored Stage 8 schedule except slickwater replaces CMHPG for direct fluid comparison. During field execution, treating pressure increased continuously and a near-screenout occurred, resulting in about 32% of planned proppant being cut out from the design. 730632 lbs of proppant were placed in formation on Stage 9. As a result of this limitation but with realistic upper bound on slickwater performance, a modified slickwater schedule (Table B2, Appendix B) was used in the simulations.

Crosslinked CMHPG Treatment Schedule 2 (Table B3, Appendix B) is identical in size and pumping sequence as modified slickwater schedule and was included to allow direct fluid system comparison (Section 5.4) and treatment size evaluation (Section 5.6).

5. RESULTS AND DISCUSSION

Table 2. Summary of fracture hits at offset wells 16A(78)-32 and 16B(78)-32 for all simulated scenarios

Scenario	Case	Frac Hits on 16A	Frac Hits on 16B
Scenario A: Match 16A Lateral	CMHPG	32	51
	CMHPG with Prior Frac	21	25
	Slickwater	35	58
	Slickwater with Prior Frac	18	34
Scenario B: Match Mid-level	CMHPG	26	49
	CMHPG with Prior Frac	15	29
	Slickwater	21	59
	Slickwater with Prior Frac	8	33
Scenario C: Match 16B Lateral	CMHPG	19	40
	CMHPG with Prior Frac	9	28
	Slickwater	5	51
	Slickwater with Prior Frac	0	26

Table 2 summarizes cumulative fracture hit response at offset wells 16A(78)-32 and 16B(78)-32 for all simulation sensitivity cases with 3 lateral alignment, 2 stimulation fluid systems, along with conditions with and without stimulation from 2024 FORGE campaign. The results show that fracture connectivity is strongly controlled by vertical and lateral placement, stimulation fluid rheology, stress and permeability changes, emphasizing the importance of integrated trajectory and stimulation design in multi-well EGS development.

5.1 Scenario A – Well 16C(78)-32 aligned with Well 16A(78)-32

Scenario A evaluates stimulation performance when the lateral of Well 16C(78)-32 is aligned with the elevation of Well 16A(78)-32. Fracture hits to Wells 16A(78)-32 and 16B(78)-32 were used as a proxy of hydraulic connectivity and fracture reach. Stage 1 (toe) has a lateral separation of approximately 281 ft, while Stage 20 (heel) has a lateral separation of approximately 603 ft. This trajectory configuration enables assessment of distance dependent connectivity under different stimulation conditions (see Appendix A, Figure A1).

5.1.1 Crosslinked CMHPG treatment without prior stimulation

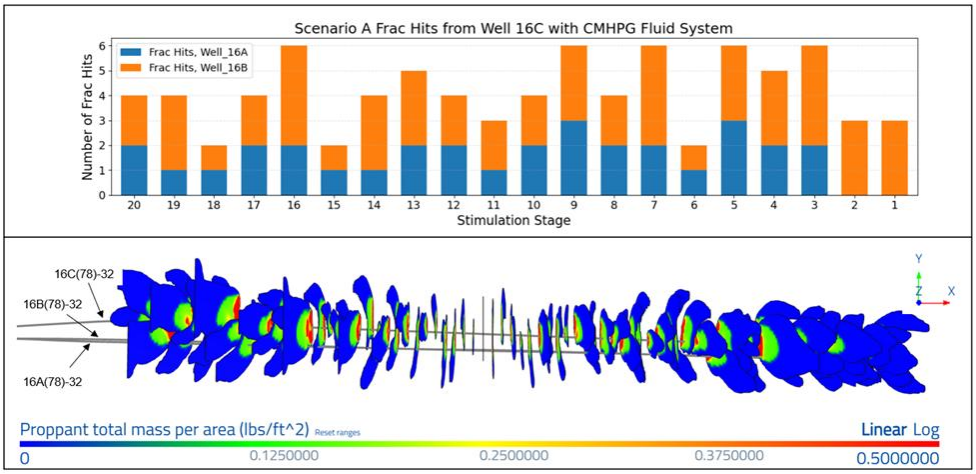

Figure 5. Scenario A fracture connectivity to Wells 16A(78)-32 and 16B(78)-32 with crosslinked CMHPG treatment without prior stimulation.

In Scenario A with crosslinked CMHPG fracturing fluid (Figure 5), 80 potential hydraulic fractures were initiated from Well 16C(78)-32, representing the maximum number of fractures that can intersect the offset wells. Of these, 32 fractures intersected Well 16A(78)-32 and 51 fractures intersected Well 16B(78)-32, corresponding to 40% and 64% of the initiated fractures, respectively. Although Well 16C is elevation-matched to Well 16A, fracture intersections occur more frequently at Well 16B which is located 300 ft above 16A. This suggests that fracture connectivity in Scenario A is not limited to elevation alignment but instead exhibits a preference for hydraulic communication with the upper offset well under crosslinked CMHPG treatment.

Stage-by-stage fracture hit results show that interwell connectivity is most often obtained at intermediate closure distances (about 350–420 ft) where total fracture hit counts are highest and intersections with both offset wells are common. At larger closure distances near the heel fracture intersections with Well 16A decrease, and Well 16B continues to have higher hit count across most stages. Overall

fracture hit distribution shows that Scenario A with CMHPG supports sustained interwell connectivity at all closure distances and a bias towards preference with Well 16B.

5.1.2 Slickwater treatment without prior stimulation

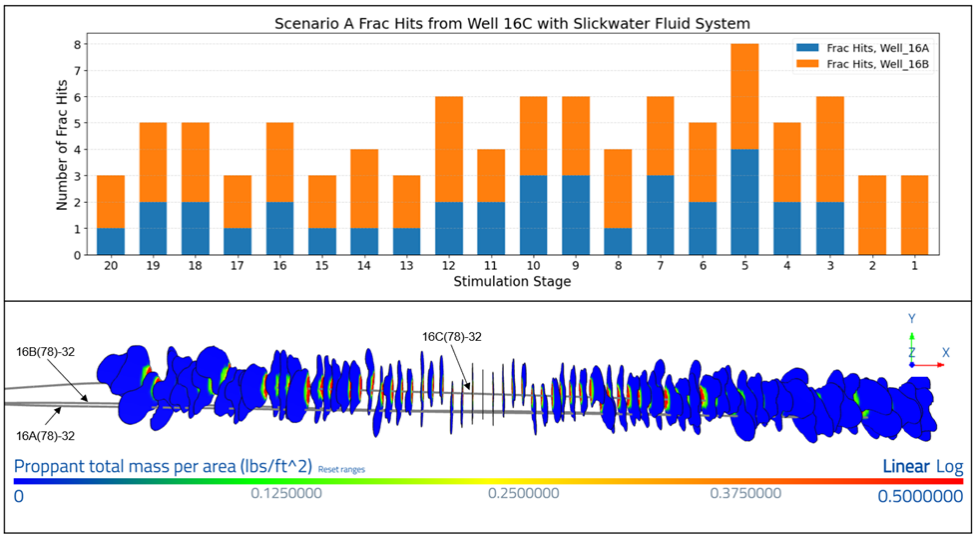

Figure 6. Scenario A fracture connectivity to Wells 16A(78)-32 and 16B(78)-32 with slickwater treatment without prior stimulation.

For the slickwater treatment in Scenario A (Figure 6), fracture intersections are broadly distributed across the stimulated area, with 35 fractures intersecting Well 16A(78)-32 and 58 intersecting Well 16B(78)-32, representing 44% and 73% of 80 initiated fractures, respectively. Higher intersection frequency at Well 16B is retained. Compared to CMHPG, slickwater yields more fracture intersections at both offset wells than CMHPG case.

The stage-resolved fracture hit distribution shows that connectivity is most effective over intermediate closure distances between 350–420 ft. In the stimulated interval, intersections with Well 16A remain variable, while connectivity with Well 16B remains constant.

5.1.3 Crosslinked CMHPG treatment with prior 2024 stimulation

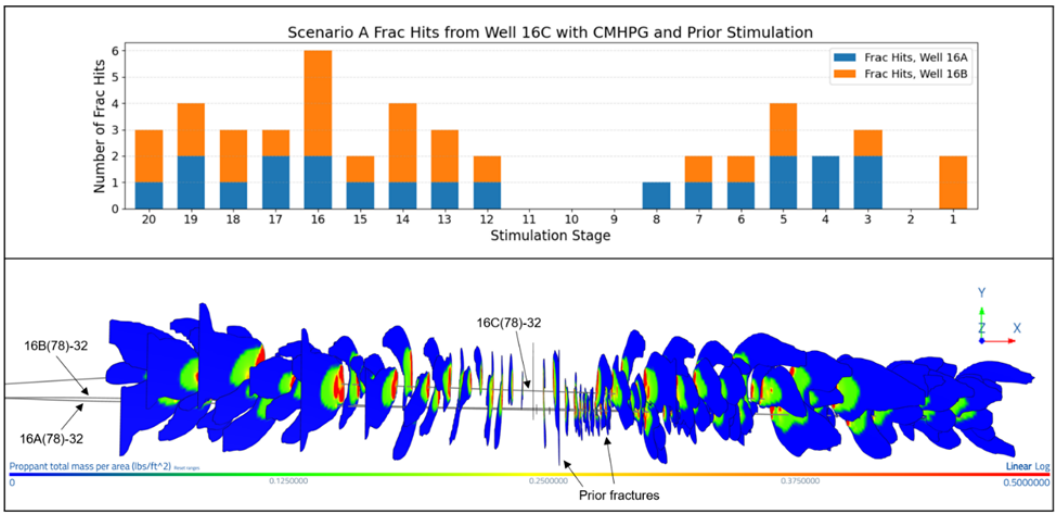

Figure 7. Scenario A fracture connectivity to Wells 16A(78)-32 and 16B(78)-32 with crosslinked CMHPG treatment and prior stimulation.

In Scenario A, the crosslinked CMHPG treatment with prior stimulation from the 2024 FORGE campaign (Figure 7) demonstrates a clear reduction in counted interwell connectivity compared with the unstimulated CMHPG base case. The number of fractures intersecting wells decreases to 21 hits at Well 16A(78)-32 and 25 hits at Well 16B(78)-32 versus 32 and 51 hits respectively for the unstimulated scenario, suggesting that prior stimulation alters local stress state and fracture propagation pathways, which limits the formation of new hydraulic fractures from Well 16C(78)-32 intersecting the offset wells.

It is important to note that the reported fracture hit counts may underestimate the effective hydraulic connectivity. In the ResFrac simulations, only newly created hydraulic fractures intersecting the offset wells are counted as fracture hits. Reactivated connections through pre-existing fractures generated during the 2024 stimulation campaign are not counted as fracture hits. Thus, fracture reactivation pathways connecting Well 16C(78)-32 to Well 16A(78)-32 or 16B(78)-32 are not counted in the reported fracture hit counts.

Despite the overall decrease in counted connectivity, fracture intersections are more frequent at Well 16B(78)-32, suggesting that the preferred hydraulic connection to the upper lateral persists even in stress shadowed conditions. Stage-by-stage fracture hit results show that prior stimulation effects are most pronounced from toe to approximately Stage 11. In particular, Stage 2, 9, 10 and 11 have no new fracture intersection with either offset well, consistent with localized suppression of fracture growth caused by stimulation-induced stress shadowing. Beyond this interval, fracture intersections resume towards the heel, but at a lower frequency than in the unstimulated case.

This sensitivity study assumes a three-year shut-in period between 2024 stimulation and the Well 16C(78)-32 treatment, consistent with Utah FORGE field operations. Accordingly, the modeled stress shadow effects reflect long-term stress redistribution rather than short-term stimulation interference, while the fracture hit metric reflects only new fracture creation rather than reactivated connectivity.

5.1.4 Slickwater treatment with prior 2024 stimulation

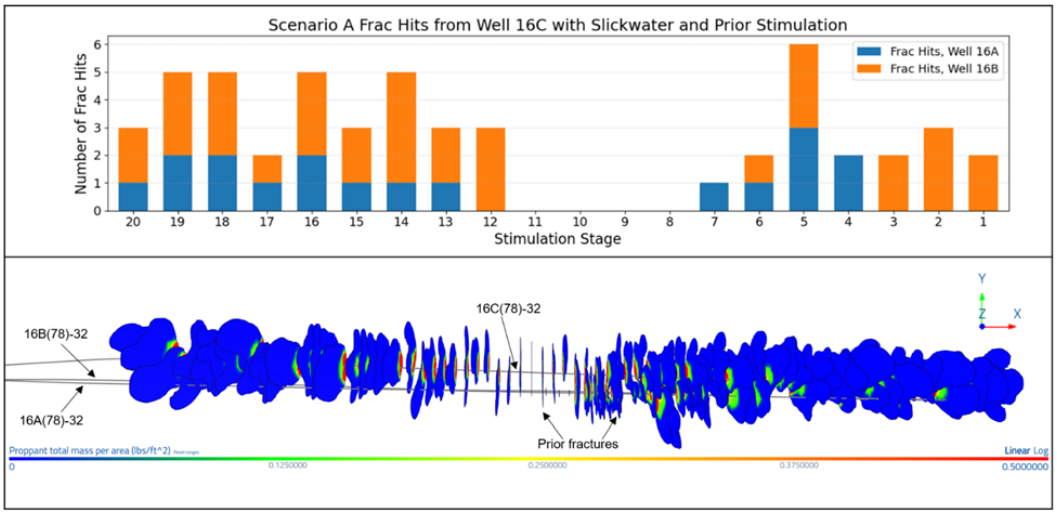

Figure 8. Scenario A fracture connectivity to Wells 16A(78)-32 and 16B(78)-32 with slickwater treatment and prior stimulation.

In Scenario A, the slickwater treatment with prior stimulation (Figure 8) shows notably lower interwell connectivity than the unstimulated slickwater case. Fracture intersections are reduced to 18 hits at Well 16A(78)-32 and 34 hits at Well 16B(78)-32, which represent 23% and 43% of the 80 initiated fractures, respectively. The number of fracture hits count may underestimate the effective interwell hydraulic connectivity because the reactivated fracture connections between Well 16C(78)-32 to the offset wells are not reflected in the reported hit numbers.

Despite the overall reduction in counted connectivity, fracture intersections remain more frequent at Well 16B(78)-32. Compared to CMHPG treatment with prior stimulation, slickwater results in less intersections at Well 16A, but more intersections at Well 16B, showing stronger asymmetry in interwell connectivity under low viscosity conditions.

Stage-by-stage fracture hit results show that the effects of prior stimulation are most severe in a stress shadowed interval from toe to about Stage 11. Stages 8 through 11 show no fracture intersection with either offset well, consistent with localized suppression of fracture growth caused by previous stimulation stress shadowing. Outside this stress shadowed interval, fracture intersections resume but are unevenly distributed along the lateral and are dominated by connectivity to Well 16B(78)-32.

Relative to CMHPG with prior stimulation, slickwater maintains higher fracture hit frequencies at the upper offset well but lacks continuity in multiwell connectivity towards Well 16A(78)-32. This means that under stress shadowed conditions, slickwater can still promote fracture propagation towards the upper lateral but fails to sustain distributed and symmetric interwell connectivity over the prior stimulated interval. Given the complexity of the Utah FORGE fracture network created by prior stimulation, effective hydraulic connectivity between Well 16C(78)-32 and Wells 16A(78)-32 and 16B(78)-32 in the slickwater Scenario A case may be underestimated, as reactivated pre-existing fracture pathways are not captured by the fracture hit measurement.

5.2 Scenario B – Well 16C(78)-32 at mid-level between 16A(78)-32 and 16B(78)-32

Scenario B evaluates stimulation when Well 16C(78)-32 is situated mid-level between Wells 16A(78)-32 and 16B(78)-32, thus yielding a more symmetric geometric relationship to the offset wells than Scenario A. Across all stages, Stage 1 (toe) corresponds to an approximate 278 ft lateral separation distance and Stage 20 (heel) corresponds to an approximate 599 ft lateral separation distance, enabling evaluation of distance-dependent fractures to reach the earlier wells under balanced vertical alignment (see Appendix A, Figure A2).

5.2.1 Crosslinked CMHPG treatment without prior stimulation

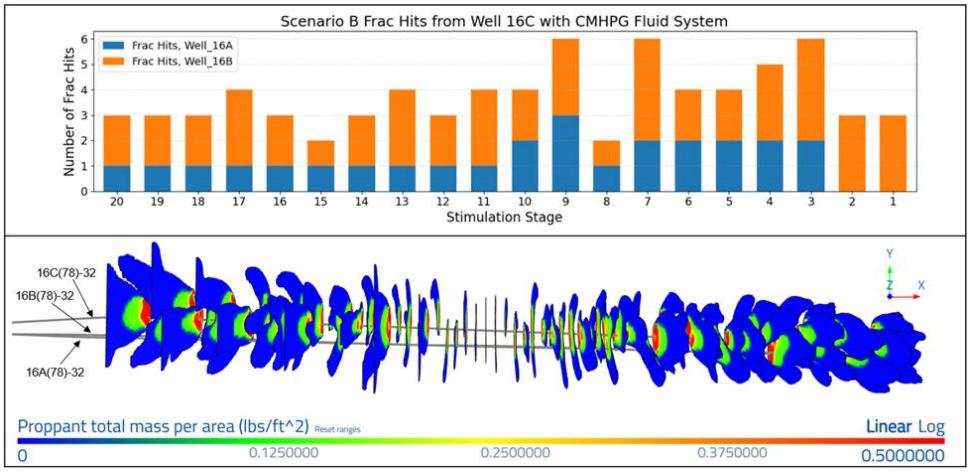

Figure 9. Scenario B fracture connectivity to Wells 16A(78)-32 and 16B(78)-32 with crosslinked CMHPG treatment without prior stimulation.

For the crosslinked CMHPG treatment in Scenario B(Figure 9) the stage-by-stage fracture hit distribution indicates sustained connectivity to both offset wells across most stages. In total, Scenario B with CMHPG generates 26 fracture hits on Well 16A(78)-32 and 49 fracture hits on Well 16B(78)-32, suggesting strong communication between the wells, with preference to the upper well. Toe-side stages generally have higher intersection frequency due to lower propagation distance requirements. Measurable connectivity persists through many heel-side stages, consistent with CMHPG's ability to retain fracture width and transport proppant under increasing separation.

Relative to Scenario A CMHPG base case, Scenario B shows a notable reduction in connectivity to Well 16A(78)-32 (26 vs. 32 hits) and a slight reduction to Well 16B(78)-32 (49 vs. 51 hits).This suggests that although mid-level placement improves vertical symmetry, the overall connectivity response remains strongly affected by fracture propagation dynamics, particularly the preferential upwards growth tendency.

5.2.2 Slickwater treatment without prior stimulation

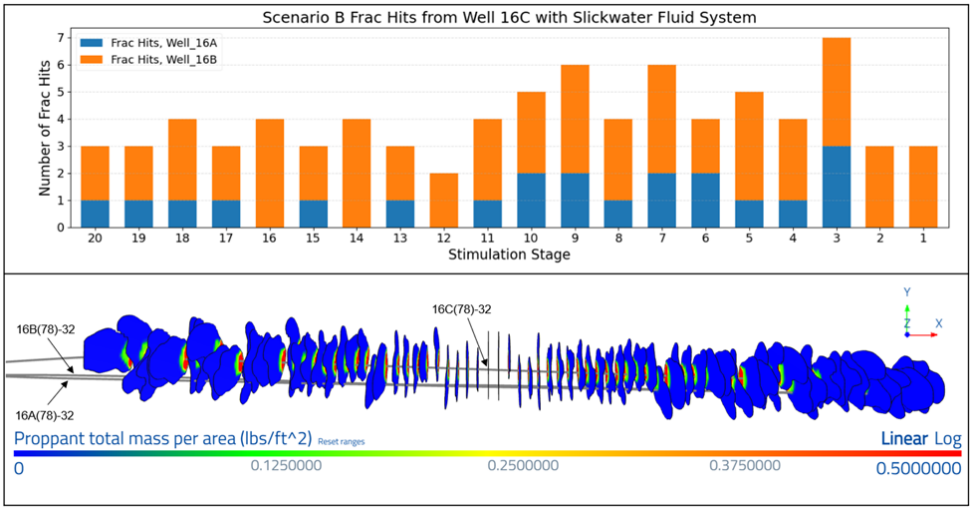

Figure 10. Scenario B fracture connectivity to Wells 16A(78)-32 and 16B(78)-32 with slickwater treatment without prior stimulation.

Scenario B slickwater stimulation fracture hit response (Figure 10) is strongly biased towards the upper well. Scenario B records 21 fracture hits on Well 16A(78)-32 and 59 hits on Well 16B(78)-32, which suggests fractures intersect the upper well far more frequently. Along the lateral, toe-side stages exhibit more frequent fracture intersections, whereas heel-side stages show more selective connectivity as the distance to the offset wells increases.

Relative to Scenario A with slickwater (35 hits on 16A(78)-32 and 58 hits on 16B(78)-32), Scenario B shows significant reduction in connectivity to Well 16A(78)-32, while connectivity to Well 16B(78)-32 remains essentially unchanged. It appears that mid-level placement alone is not sufficient to compensate for the limitations of slickwater, which produces narrower fractures and less proppant

support as propagation distance increases. The proppant mass distribution supports this interpretation, with discontinuous, localized fracture support and connectivity dominated by pathways towards the upper well. Overall, it appears that for slickwater treatment, interwell connectivity is governed primarily by fracture-width sustainability and 3-dimensional propagation behavior rather than vertical symmetry alone, which suggests the need for improved fluid rheology or alternative design strategies to achieve balanced connectivity in Scenario B.

5.2.3 Impact of prior stimulation on fracture connectivity in Scenario B

For the crosslinked CMHPG cases in Scenario B, the 2024 FORGE stimulation reduces the fracture connectivity at both offset wells. Fracture hits at Well 16A(78)-32 decrease from 26 to 15 (42% reduction) and hits at Well 16B(78)-32 decrease from 49 to 29 (41% reduction). The nearly proportional decrease at both wells indicates stress shadowing which restricted the new fracture growth upward and downward.

In contrast, the slickwater cases are more sensitive to previous stimulation. Fracture hits to Well 16A(78)-32 decrease from 21 to 8 (62% reduction) and hits to Well 16B(78)-32 reduce from 59 to 33 (44% reduction), suggesting a more severe loss of connectivity than CMHPG. The reduction is particularly severe at the lower offset well due to low-viscosity slickwater unable to propagate new fractures through stress-modified rock and to establish intersections under these conditions.

Given the structurally complex fracture system established by previous FORGE stimulation, the loss of connectivity in the Scenario B should be interpreted as a conservative estimate. Parts of the hydraulic communication between Well 16C(78)-32 and offset wells may occur through prior stimulated fracture segments that are reactivated during the treatment but not included in the reported intersection count. As a result, the fracture hit metric primarily captures only the formation of new fracture pathways rather than the full extent of hydraulic linkage. Even with this consideration, the results show that slickwater is more constrained by stress-altered conditions than CMHPG and hence, fluid rheology is crucial when designing re-stimulation or infill strategies in EGS reservoirs.

5.3 Scenario C – Well 16C(78)-32 aligned with Well 16B(78)-32

Scenario C evaluates stimulation behavior when Well 16C(78)-32 is vertically aligned with Well 16B(78)-32 (upper well). Along the lateral, Stage 1 (toe) corresponds to an approximate 275 ft lateral separation distance, and Stage 20 (heel) corresponds to an approximate 602 ft lateral separation distance, thus allowing analysis of fracture reach for different separations (see Appendix A, Figure A3).

5.3.1 Crosslinked CMHPG treatment without prior stimulation

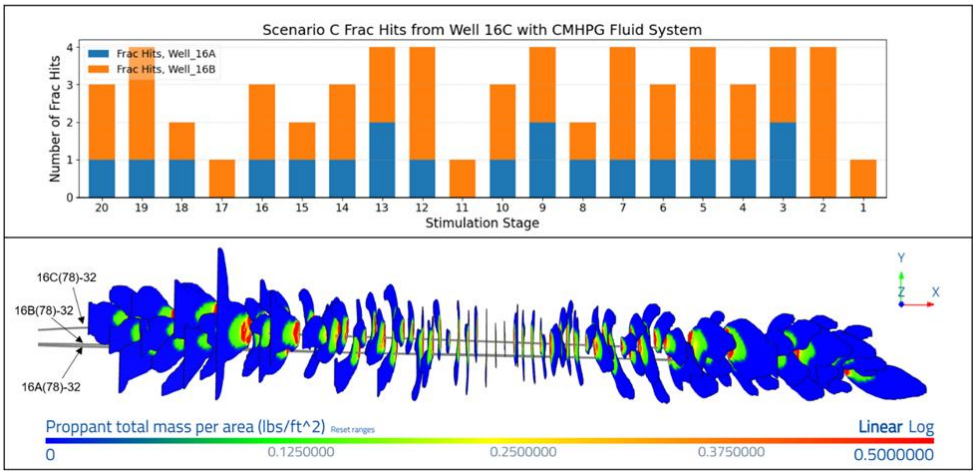

Figure 11. Scenario C fracture connectivity to Wells 16A(78)-32 and 16B(78)-32 with crosslinked CMHPG treatment without prior stimulation.

For Scenario C with crosslinked CMHPG fluid system (Figure 11), the total fracture hit count is 19 hits on Well 16A(78)-32 and 40 hits on Well 16B(78)-32, indicating sustained but asymmetric interwell connectivity.

Relative to Scenario A and B, Scenario C shows the lowest overall connectivity to both wells for the CMHPG cases, with the largest reduction to the lower well. Fracture hits at Well 16A(78)-32 decrease from 32 (Scenario A) and 26 (Scenario B) to 19 (Scenario C), while hits at Well 16B(78)-32 decrease from 51 (Scenario A) and 49 (Scenario B) to 40 (Scenario C).This indicates that vertical placement strongly controls connectivity distribution: alignment with the upper well improves preferential intersection of Well 16B(78)-32 and suppresses downward fracture growth toward Well 16A(78)-32, particularly at the heel-side with large lateral separation distances. These results show that although CMHPG maintains fracture width and multi-well connectivity, trajectory placement remains a dominant control on interwell connectivity balance, with mid-level placement (Scenario B) providing more symmetry than either of the vertically biased configurations.

5.3.2 Slickwater treatment without prior stimulation

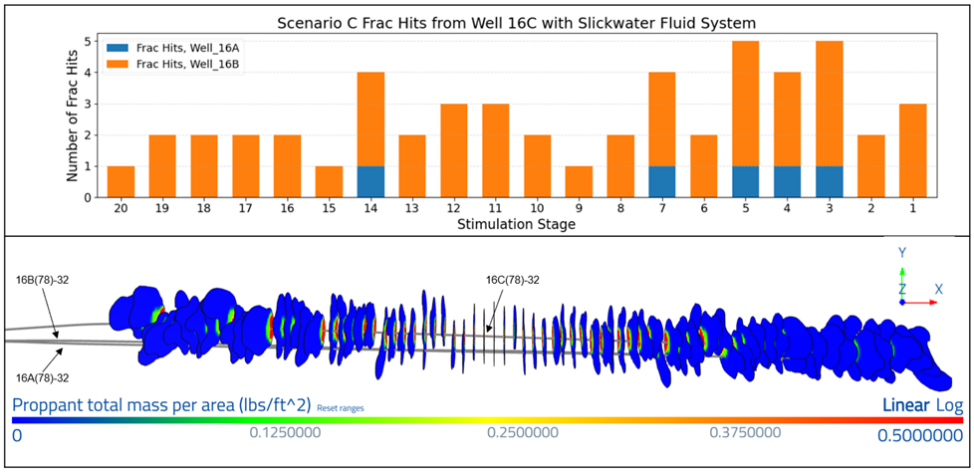

Figure 12. Scenario C fracture connectivity to Wells 16A(78)-32 and 16B(78)-32 with slickwater treatment without prior stimulation.

In Scenario C slickwater stimulation (Figure 12), interwell connectivity becomes very asymmetric with only 5 hits on Well 16A(78)-32 and 51 hits on Well 16B(78)-32. As the lateral separation distance increases, fracture intersections are dominated by pathways towards the upper well, and connectivity to the lower well is suppressed. Toe-side stages contribute most of the limited intersections on Well 16A(78)-32, while heel-side stages favor selective upward fracture growth, as propagation distance increases.

Compared with Scenarios A and B with slickwater (35/58 hits and 21/59 hits on Wells 16A(78)-32/16B(78)-32 respectively), Scenario C exhibits the highest connectivity imbalance and the lowest connectivity to the lower well. The dramatic reduction of Well 16A(78)-32 hits (to 5) shows that vertical alignment with the upper well inhibits downward fracture growth for low viscosity fluids. Collectively, these results show that slickwater is not able to overcome strong vertical bias in Scenario C, and trajectory placement dominates interwell connectivity.

5.3.3 Impact of prior stimulation on fracture connectivity in Scenario C

For the crosslinked CMHPG case of Scenario C, the 2024 FORGE stimulation results in a significant and asymmetric decrease of the interwell connectivity: Fracture hits at the upper well (Well 16B(78)-32) decrease from 40 to 28 (30% reduction) and hits at the lower well (Well 16A(78)-32) decrease from 19 to 9 (53% reduction). This response indicates that prior stimulation restricts downward fracture growth while still allowing some new fractures to propagate towards the vertically aligned upper well.

For the treatment of slickwater in Scenario C, the prior stimulation produces highly directional and strongly attenuated connectivity response. Fracture intersections with the lower well (Well 16A(78)-32) are completely absent, while intersections with the upper well decrease from 51 to 26 (49% reduction). This pattern indicates that slickwater cannot effectively establish new downward fracture propagation under stress-altered conditions and instead concentrates fracture growth towards the vertically aligned upper well. Comparatively with CMHPG, slickwater exhibits a more pronounced loss of connectivity and stronger directional focusing.

Given the inherited fracture network structure at Utah FORGE, the connectivity results for both the CMHPG and slickwater treatment in Scenario C represent a conservative depiction of interwell interaction. Parts of the hydraulic response could be accommodated through pre-existing fracture segments that are mobilized during stimulation but not counted to the fracture intersection metric. Thus, the reported connectivity emphasizes newly generated fracture links rather than all fluid-accessible pathways. However, we find that the slickwater in Scenario C primarily reinforces connectivity near the aligned upper well and offers limited capability to sustain vertically distributed fracture networks following prior stimulation.

5.4 Fracture connectivity cross-scenario comparison

Across all cases (Table 2), Scenario A (with Well 16C(78)-32 aligned with Well 16A(78)-32) produces the highest total fracture hit count to both offset wells with the strongest overall interwell connectivity. This trend holds for both CMHPG and slickwater and persists after incorporating the 2024 stimulation history, despite reduced absolute hit counts due to stress shadowing. Scenario B (mid-level placement) shows intermediate connectivity with better distribution between Wells 16A(78)-32 and 16B(78)-32 but lower magnitudes than Scenario A. Scenario C (with Well 16B(78)-32 aligned) has the most asymmetric response strongly favoring the upper well and limited or eliminated connections to lower Well, especially for slickwater.

Fluid system choice also influences placement effects. Table B4 (Appendix B) summarizes the CMHPG–slickwater comparison under an identical treatment schedule for the three trajectory scenarios. In Scenario A (match 16A lateral), slickwater produces slightly more fracture hits than CMHPG at both wells (35 vs. 31 on 16A; 58 vs. 47 on 16B), indicating a broader hydraulic reach while maintaining the same preference to the upper well. In Scenario B (mid-level placement), CMHPG provides higher connectivity to the lower well (24 vs.

21 on 16A), whereas slickwater achieves highest connectivity to the upper well (59 vs. 46 on 16B), showing a stronger upward bias under low viscosity conditions. The contrast is most significant in Scenario C (match 16B lateral), where slickwater becomes highly asymmetric (5 hits on 16A; 51 on 16B) compared with CMHPG (18 hits on 16A; 38 on 16B), suggesting CMHPG can sustain connectivity to the lower well while slickwater preferentially concentrates connectivity towards the upper lateral. Overall, under identical pumping schedules, slickwater tends to maximize intersections with Well 16B, while CMHPG more consistently supports balanced multiwell connectivity, especially when matching mid-level or upper-lateral trajectories.

5.5 Proppant settlement effects

To compare proppant distribution patterns between Scenario A and B, Stage 9 interval located near the lateral center was selected for detailed evaluation. The Stage 9 CMHPG proppant mass distributions (Figure 13) suggest distinct long-term circulation behavior between Scenario A and Scenario B. This contrast reflects differences in the location and continuity of proppant-supported fracture apertures connected to the wellbores, which govern post-shut-in conductivity and stability during pressure and thermal cycling. In Scenario A, an effective propped tie-in is developed near Well 16A(78)-32, whereas Well 16B(78)-32 lacks a clearly established proppant-supported connection. As a result, the primary flow path between wells 16C(78)-32 and 16A(78)-32 is expected to remain relatively stable during circulation. In contrast, flow communication toward Well 16B(78)-32 relies on unpropped or weakly propped fracture segments, which are less mechanically robust. These segments are more sensitive to increasing effective stress, limiting the persistence of hydraulic connectivity to 16B(78)-32 during long-term circulation. Consequently, sustained flow to and from 16B(78)-32 may be reduced, with circulation increasingly dominated by the better supported flow pathway toward 16A(78)-32.

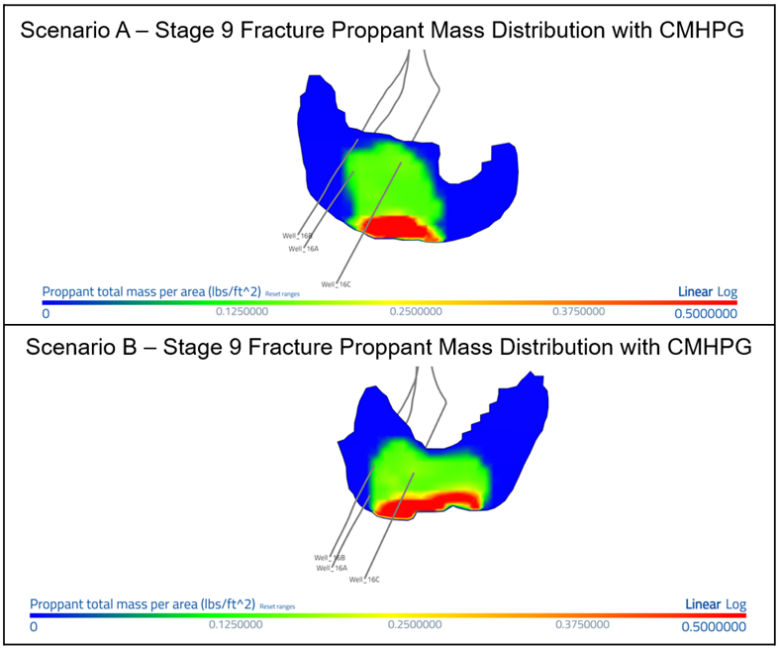

Figure 13. Comparison of CMHPG proppant distribution and wellbore connectivity within Stage 9 fracture for Scenario A and B

In contrast, for Scenario B, the proppant settlement pattern more effectively covers the fracture network between 16C(78)-32, 16A(78)-32, and 16B(78)-32, forming mechanically supported, multi-well-connected pathways. This is generally more suitable for long-term circulation. Propped connections can preserve fracture width and conductivity, stabilize injectivity and productivity, and reduce sensitivity to stress and temperature transients. The flow field is more distributed, sweep efficiency is better. Overall, unlike Scenario A, the Stage 9 proppant distribution in Scenario B can provide a better controllable long-term circulation response.

The Stage 9 slickwater proppant mass distributions (Figure 14) show that both Scenarios A and B are characterized by localized proppant accumulation near the injection well (16C(78)-32) and limited lateral and vertical proppant transport away from the wellbore. In Scenarios A and B, the proppant pack is concentrated near the injection well (16C(78)-32) and fails to establish effective propped connection with either offset well, particularly Well 16B(78)-32. Long-term circulation would result in a weakly supported fracture network relying on unpropped or poorly propped fracture segments to flow toward production wells. These fracture segments are highly susceptible to lateral separation under increasing effective stress, leading to conductivity loss, unstable pressure response and decreased circulation efficiency, making sustained and interpretable circulation performance difficult to maintain.

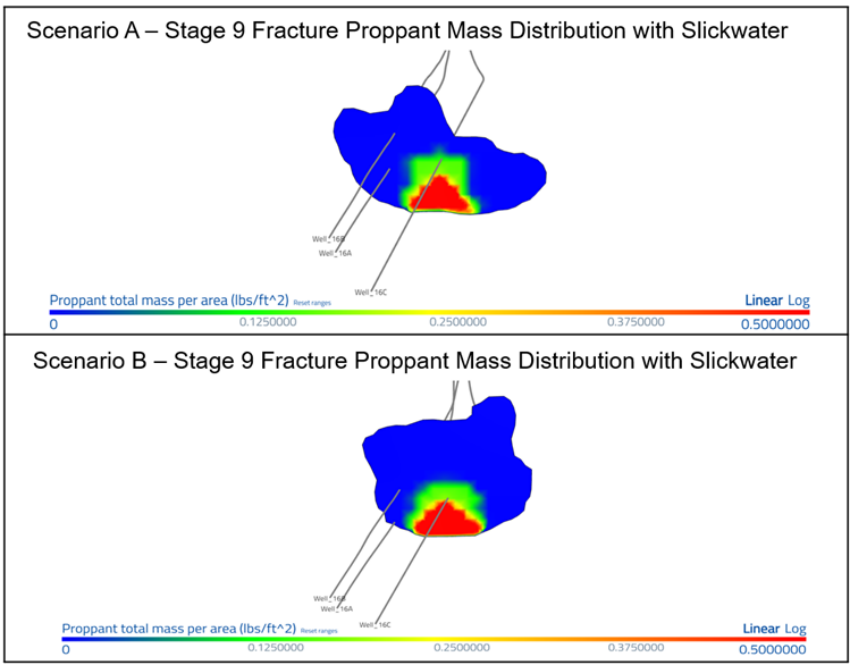

Figure 14. Comparison of slickwater proppant distribution and wellbore connectivity within Stage 9 fracture for Scenario A and B

5.6 Treatment size effects

The Stage 9 proppant mass distributions of Scenario B (Figure 15) highlight the effects of treatment size on fracture support and interwell connectivity under crosslinked CMHPG stimulation. Larger treatment (CMHPG Schedule 1; top panel) produces a larger propped region which spans the interwell space and reaches both offset wells 16A(78)-32 and 16B(78)-32. Proppant is distributed continuously across the central fracture zone, high concentrations concentrated near the Well 16C wellbore and persistent proppant presence extending laterally toward both offset wells. Smaller treatment (CMHPG Schedule 2; bottom panel) produces a more localized propped zone near Well 16C with proppant coverage diminishing before reaching either offset well. Although fracture geometry is established in both cases, the smaller treatment size limits the propped area and results in unpropped or weakly propped fracture segments towards offset wells.

These differences in the proppant distribution have important implications for long-term circulation. In larger treatment, continuous proppant supported paths between injection well and both offset wells are more likely to be conductive under increasing effective stress, allowing distributed flow and stable multiwell circulation. By contrast, the smaller treatment results in fracture connectivity relies on partially or entirely unpropped segments near offset wells and is more susceptible to closure and conductivity loss over time. These results show that even in the same fluid system treatment size plays a key role in proppant supported connectivity and long-term EGS circulation.

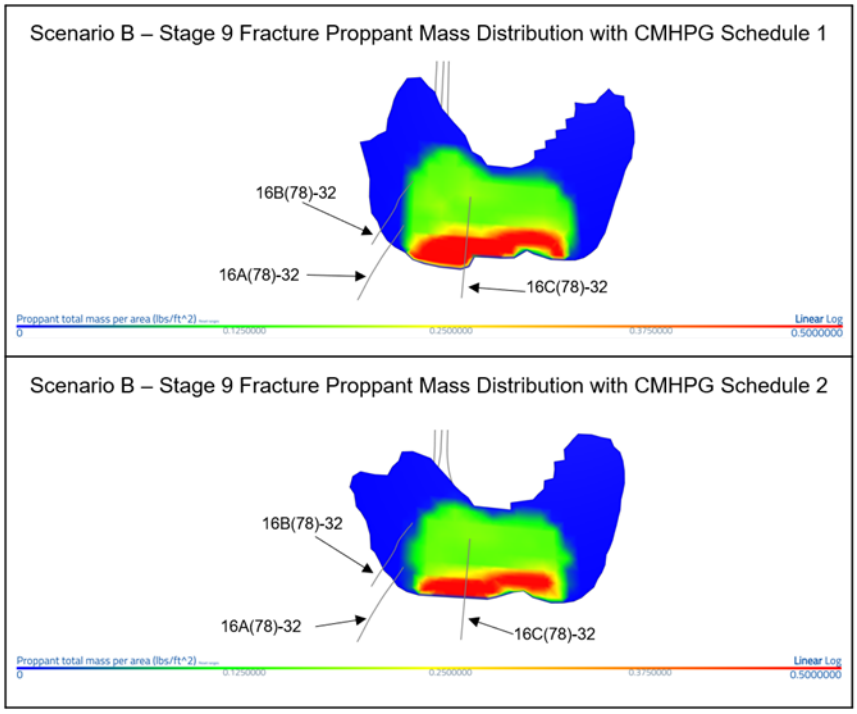

Figure 15. Effect of treatment size on Stage 9 proppant mass distribution in Scenario B using crosslinked CMHPG: (top) larger treatment (Table B1, Appendix B), (bottom) smaller treatment (Table B3, Appendix B)

6. DESIGN IMPLICATION FOR WELL 16C(78)-32

Based on the integrated analysis of fracture connectivity, proppant settlement behavior, and sensitivity to prior stimulation, several key implications emerge for the drilling and stimulation design of Well 16C(78)-32.

Trajectory selection.

A mid-level position between Well 16A(78)-32 and 16B(78)-32 (Scenario B) is the most balanced and resilient fracture connection. This position promotes bidirectional hydraulic communication, reduces sensitivity to lateral separation distance, and avoids vertically biased or single-sided fracture networks. In comparison with Scenario A and C, Scenario B is more robust for long-term circulation testing.

Stimulation fluid selection.

Crosslinked CMHPG is strongly preferred for Well 16C(78)-32 stimulation. CMHPG, or a synthetic polymer with more thermal tolerance, is the most robust in all scenarios. There is resistance to stress shadowing, better proppant transport and the capability of a larger treatment design resulting in better well-to-well connectivity. In contrast, slickwater treatments yield localized and discontinuous proppant placement that is highly susceptible to lateral separation and connectivity degradation during long-term circulation and thermal cycling.

Proppant Connections and Circulation stability.

Propped connections to offset wellbores are the first order control of circulation stability. Scenario B with CMHPG provides mechanically supported connections between all three wells (16C(78)-32–16A(78)-32–16B(78)-32), enabling stable injectivity, distributed flow and more interpretable thermal and pressure responses. Configurations without effective propped connections have a higher risk of progressive conductivity loss during extended testing.

Future Testing Flexibility.

The proposed design, Scenario B with CMHPG, allows for the most flexibility for future testing, such as potential stimulation from Well 16B(78)-32 with proppant to improve multiwell connectivity for long-term circulation, reversed flow circulation, staged stimulation sequencing, and long-duration thermal sweep evaluation. A mechanically supported fracture network (propped) increases confidence that observed responses reflect reservoir behavior rather than progressive fracture degradation.

7. CONCLUSIONS

This work evaluates fracture connectivity for the stimulation of Well 16C(78)-32 proposed at Utah FORGE using a structured sensitivity analysis considering the effect of lateral placement, stimulation fluid system and stimulation history from the 2024 FORGE campaign.

Fracture hit responses at offset wells 16A(78)-32 and 16B(78)-32 are used as a proxy for hydraulic connectivity, comparing three trajectory scenarios and two fluid systems.

The results show that vertical (elevation) well placement is the primary control on interwell connectivity. A mid-level trajectory between Wells 16A(78)-32 and 16B(78)-32 yields the most balanced and resilient fracture networks, while alignment with a single offset well leads to asymmetric, stress sensitive connectivity. Stimulation fluid selection also influences this behavior. Crosslinked CMHPG provides more balanced and durable interwell connectivity under both unstimulated and stimulated stress conditions. Although slickwater can generate higher fracture hit count in Scenario A, its connectivity is more asymmetric in Scenario B and C and limited by stimulation size.

Proppant settlement suggests that the spatial stability of proppant-supported fracture segments plays a key role in controlling potential interwell connectivity. Scenario B with CMHPG establishes continuous propped pathways between wells and tend to have more distributed proppant placement and reduce reliance on isolated fracture segments. Large treatment designs with crosslinked CMHPG can improve interwell connectivity. Slickwater treatment tends to have more localized and discontinuous proppant distributions and are more sensitive to stress shadowing and fracture closures, especially in the presence of prior stimulation.

Overall, the findings support a mid-level trajectory for Well 16C(78)-32 combined with a crosslinked CMHPG stimulation strategy as the most robust design for future FORGE EGS development. This configuration maximizes interwell connectivity, enhances operational flexibility and reduces uncertainty in long-term circulation testing, providing a practical framework for reliable multi-well EGS reservoir development.

ACKNOWLEDGEMENTS

Funding for the Utah FORGE project was provided by the U.S. Department of Energy. The authors gratefully acknowledge the extensive technical support provided by the ResFrac team throughout the development and calibration of the numerical models used in this study. Special thanks are extended to Christopher Ponners, whose technical guidance was critical to the calibration and validation of the simulation models.

REFERENCES

[1] Asai, P., Panja, P., Velasco, R., McLennan, J., & Moore, J. (2018). Fluid flow distribution in fractures for a doublet system in Enhanced Geothermal Systems (EGS). *Geothermics*, *75*, 171–179. https://doi.org/10.1016/j.geothermics.2018.05.005

[2] England, K., Li, P., Xing, P., Moore, J., McLennan, J., 2025. 2024 Enhanced Geothermal System Hydraulic Fracturing Campaign at Utah FORGE. Woodlands, Texas, USA. In: Presented at the SPE Hydraulic Fracturing Technology Conference and Exhibition held; 2025. SPE-223519-MS. [February] https://doi.org/10.2118/223519-MS.

[3] McClure, M., 2023. Calibration Parameters Required to Match the Utah FORGE 16A(78)-32 Stage 3 Stimulation with a Planar Fracturing Model. Stanford, California, USA. In: Presented at the 48th Workshop on Geothermal Reservoir Engineering Stanford University held; 2023. SGP-TR-224 [February].

[4] McClure, M.W., Irvin, R., England, K., McLennan, J., 2024. Numerical Modeling of Hydraulic Stimulation and Long-Term Fluid Circulation at the Utah FORGE Project. Stanford, California, USA. In: Presented at the 49th Workshop on Geothermal Reservoir Engineering Stanford University held; 2024. SGP-TR-227 [February].

[5] Moore, J., McLennan, J., Pankow, K., Finnila, A., Dyer, B., Karvounis, D., Bethmann, F., Podgorney, R., Rutledge, J., Meir, P., Xing, P., Jones, C., Barker, B., Simmons, S., Damjanac, B., 2023. Current Activities at the Utah Frontier Observatory for Research in Geothermal Energy (FORGE): A Laboratory for Characterizing, Creating and Sustaining Enhanced Geothermal Systems. Atlanta, Georgia, USA. In: Presented at the 57th US Rock Mechanics/Geomechanics Symposium held; 2023. ARMA 23–749 [June] https://doi.org/10.56952/ARMA-2023-0749.

[6] Moore, J., McLennan, J., Pankow, K., Simmons, S., Podgorney, R., Wannamaker, P., Jones, C., Rickard, W., Xing, P., 2020. The Utah Frontier Observatory for Research in Geothermal Energy (FORGE): A Laboratory for Characterizing, Creating and Sustaining Enhanced Geothermal Systems. Stanford, California, USA. In: Presented at the 45th Workshop on Geothermal Reservoir Engineering Stanford University held; 2020. SGP-TR-216 [February].

[7] Podgorney, R., Munday, L., Liu, J., Jiang, W., Finnila, A., Damjanac, B., Xing, P., & Radakovic-Guzina, Z. (2023). Thermal-Hydraulic-Mechanical (THM) Modeling of Fluid Flow and Heat/Tracer Transport Between Injection and Production Wells at the Utah FORGE Site. *Proceedings, 48th Workshop on Geothermal Reservoir Engineering Stanford University, Stanford, California*.

[8] ResFrac. https://www.resfrac.com/

[9] U.S. Department of Energy. (2019). GeoVision: Harnessing the Heat Beneath Our Feet. DOE/EE-1306. https://www.energy.gov/eere/geothermal/downloads/geovision-harnessing-heat-beneath-our-feet

[10] Xing, P., Damjanac, B., Radakovic-Guzina, Z., Torres, M., Finnila, A., Podgorney, R., Moore, J., McLennan, J., 2022. Numerical Simulation of Stimulations at the Utah FORGE Site Using the Designed Pumping Schedules. GRC Transactions 46: 618-628.

[11] Xing, P., England, K., Mclennan, J., Podgorney, R., & Moore, J. (2024). Analysis of Circulation Tests and Well Connections at Utah FORGE. *Proceedimgs, 49th Workshop on Geothermal Reservoir Engineering Stanford University, Stanford, California*.

APPENDIX A. MAP-VIEW WELL 16C(78)-32 DIRECTIONAL LATERAL LAYOUTS

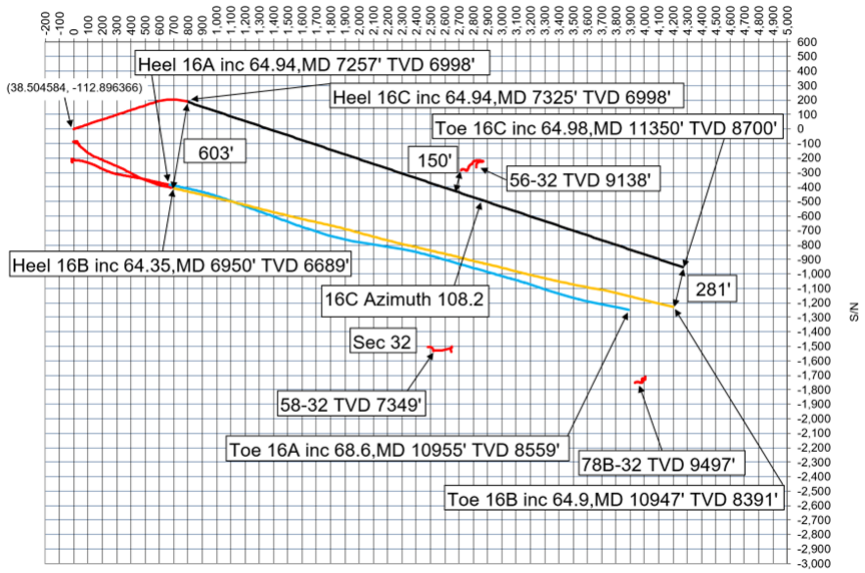

Figure A1. Scenario A Map-View Well 16C(78)-32 directional lateral layout

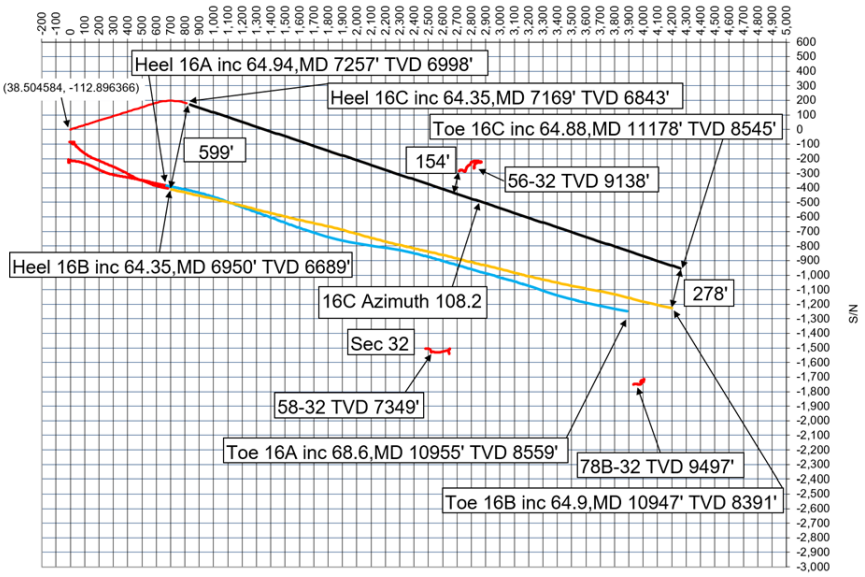

Figure A2. Scenario B Map-View Well 16C(78)-32 directional lateral layout

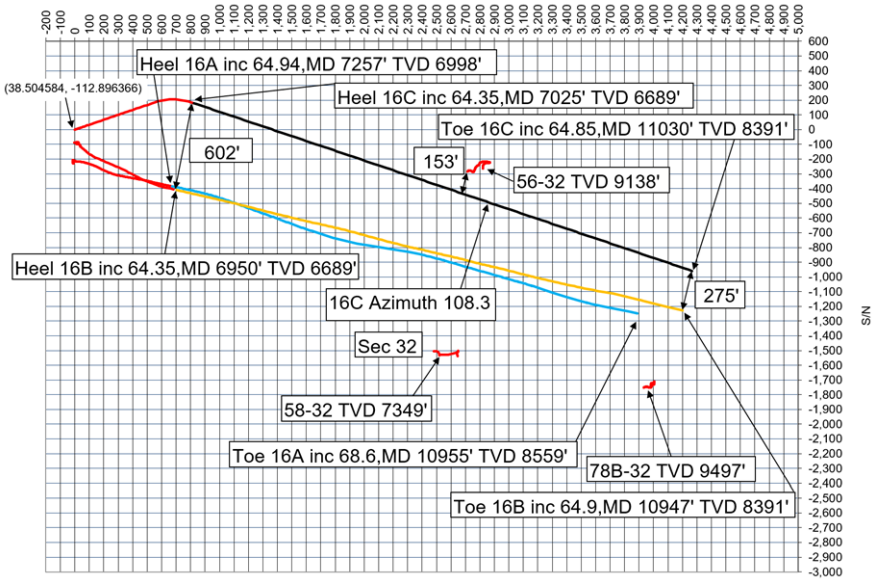

Figure A3. Scenario C Map-View Well 16C(78)-32 directional lateral layout

APPENDIX B. STIMULATION TREATMENT SCHEDULES AND RESULTS

Table B1. Crosslinked CMHPG fracturing treatment schedule (from 2024 stimulation campaign Well 16A(78)-32 Stage 8 treatment schedule)

Step Name	Step Pump Rate (bpm)	Step Fluid Volume (bbl)	Step Fluid Type	Cum Fluid Volume (bbl)	Step Prop Conc (PPA)	Step Prop Type (US mesh)	Step Prop Volume (lbm)	Cum Prop Volume (lbm)	Step Slurry Volume (bbl)	Step Pump Time (min)	Cum Pump Time (min)
Pad	80	6,400	XL CMHPG	6,400	0.00		0	0	6,400	80.0	80.0
0.5 PPA	80	3,200	XL CMHPG	9,600	0.50	100	67,200	67,200	3,273	40.9	120.9
0.75 PPA	80	3,200	XL CMHPG	12,800	0.75	100	100,800	168,000	3,309	41.4	162.3
1.00 PPA	80	6,400	XL CMHPG	19,200	1.00	100	268,800	436,800	6,690	83.6	245.9
1.00 PPA	80	6,400	XL CMHPG	25,600	1.00	40/70	268,800	705,600	6,690	83.6	329.5
1.25 PPA	80	3,200	XL CMHPG	28,800	1.25	40/70	168,000	873,600	3,381	42.3	371.8
1.50 PPA	80	3,200	XL CMHPG	32,000	1.50	40/70	201,600	1,075,200	3,418	42.7	414.5
Flush	80	350	Slickwater	32,350	0.00		0	1,075,200	350	4.4	418.9

Table B2. Slickwater fracturing treatment schedule (modified from 2024 stimulation campaign Well 16A(78)-32 Stage 9 treatment schedule)

Step Name	Step Pump Rate (bpm)	Step Fluid Volume (bbl)	Step Fluid Type	Cum Fluid Volume (bbl)	Step Prop Conc (PPA)	Step Prop Type (US mesh)	Step Prop Volume (lbm)	Cum Prop Volume (lbm)	Step Slurry Volume (bbl)	Step Pump Time (min)	Cum Pump Time (min)
Pad	80	6,400	Slickwater	6,400	0.00		0	0	6,400	80.0	80.0
0.5 PPA	80	3,200	Slickwater	9,600	0.50	100	67,200	67,200	3,273	40.9	120.9
0.75 PPA	80	3,200	Slickwater	12,800	0.75	100	100,800	168,000	3,309	41.4	162.3
1.00 PPA	80	6,400	Slickwater	19,200	1.00	100	268,800	436,800	6,690	83.6	245.9
1.00 PPA	80	6,400	Slickwater	25,600	1.00	40/70	268,800	705,600	6,690	83.6	329.5
Flush	80	350	Slickwater	25,600	0.00		0	705,600	350	4.4	333.9

Table B3. Crosslinked CMHPG fracturing treatment schedule 2 (modified from 2024 stimulation campaign Well 16A(78)-32 Stage 8 treatment schedule)

Step Name	Step Pump Rate (bpm)	Step Fluid Volume (bbl)	Step Fluid Type	Cum Fluid Volume (bbl)	Step Prop Conc (PPA)	Step Prop Type (US mesh)	Step Prop Volume (lbm)	Cum Prop Volume (lbm)	Step Slurry Volume (bbl)	Step Pump Time (min)	Cum Pump Time (min)
Pad	80	6,400	XL CMHPG	6,400	0.00		0	0	6,400	80.0	80.0
0.5 PPA	80	3,200	XL CMHPG	9,600	0.50	100	67,200	67,200	3,273	40.9	120.9
0.75 PPA	80	3,200	XL CMHPG	12,800	0.75	100	100,800	168,000	3,309	41.4	162.3
1.00 PPA	80	6,400	XL CMHPG	19,200	1.00	100	268,800	436,800	6,690	83.6	245.9
1.00 PPA	80	6,400	XL CMHPG	25,600	1.00	40/70	268,800	705,600	6,690	83.6	329.5
Flush	80	350	Slickwater	25,600	0.00		0	705,600	350	4.4	333.9

Table B4. Comparison of fracture hit responses for crosslinked CMHPG and slickwater treatment under identical stimulation schedules across Scenario A-C

Scenario	Case	Frac Hits on 16A	Frac Hits on 16B
Scenario A: Match 16A Lateral	CMHPG Schedule 2	31	47
	Slickwater	35	58
Scenario B: Match Mid-level	CMHPG Schedule 2	24	46
	Slickwater	21	59
Scenario C: Match 16B Lateral	CMHPG Schedule 2	18	38
	Slickwater	5	51